Mineral inclusions in diamonds from Karowe Mine, Botswana: super-deep sources for super-sized diamonds?

Theetso Motsamai[1] • Jeffrey W. Harris[2] • Thomas Stachel[1] • D. Graham. Pearson[1] • John Armstrong[3]

✉ T. Motsamai

motsamai@ualberta.ca

[1]Department of Earth and Atmospheric Sciences 1-26 Earth Sciences Building, Edmonton, Canada T6H 2E3.

[2] School of Geographical and Earth Sciences, Gregory Building, Glasgow, United Kingdom G12 8QQ.

[3]Lucara Diamond Corporation, Suite 2000, 885 West Georgia Street, Vancouver, Canada V6C 3E8.

Abstract

Mineral inclusions in diamonds play a critical role in constraining the relationship between diamonds and mantle lithologies. Here we report the first major and trace element study of mineral inclusions in diamonds from the Karowe Mine in north-east Botswana, along the western edge of the Zimbabwe Craton. From a total of 107 diamonds, 134 silicate, 15 oxide, and 22 sulphide inclusions were recovered. The results reveal that 53 % of Karowe inclusion-bearing diamonds derived from eclogitic sources, 44 % are peridotitic, 2 % have a sublithospheric origin, and 1 % are websteritic. The dominant eclogitic diamond substrates sampled at Karowe are compositionally heterogeneous, as reflected in wide ranges in the CaO contents (4-16 wt%) of garnets and the Mg# (69-92) and jadeite contents (14-48 mol%) of clinopyroxenes. Calculated bulk rock REE_N patterns indicate that both shallow and deep levels of the subducted slab(s) were sampled, including cumulate-like protoliths. Peridotitic garnet compositions largely derive from harzburgite/dunite substrates (~90 %), with almost half the garnets having CaO contents <1.8 wt %, consistent with pyroxene-free (dunitic) sources. The highly depleted character of the peridotitic diamond substrates is further documented by the high mean and median Mg# (93.1) of olivine inclusions. One low-Ca garnet records a very high Cr_2O_3 content (14.7 wt%), implying that highly depleted cratonic lithosphere at the time of diamond formation extended to at least 220 km depth. Inclusion geothermobarometry indicates that the formation of peridotitic diamonds occurred along a 39-40 mW/m^2 model geotherm. A sublithospheric inclusion suite is established by three eclogitic garnets containing a majorite component, a feature so far unique within the Orapa cluster. These low- and high-Ca majoritic garnets follow pyroxenitic and eclogitic trends of majoritic substitution, respectively. The origin of the majorite-bearing diamonds is estimated to be between 330 to 420 km depth, straddling the asthenosphere–transition zone boundary. This new observation of superdeep mineral inclusions in Karowe diamonds is consistent with a sublithospheric origin for the exceptionally large diamonds from this mine.

Key words:
Zimbabwe Craton
Orapa kimberlite cluster
Sublithospheric
Majorite

Introduction

The recent recovery of exceptionally large diamonds (including the 1,109 carats Lesedi la Rona) at the Karowe mine in north-eastern Botswana raises the question: what controls such an exceptionally coarse size-frequency distribution? To address this question we studied the mineralogy and chemistry of inclusions in a representative suite of diamonds from this mine.

Based on recent conflicting views on the origin of very large (typically nitrogen-free) gem diamonds, invoking either a megacryst-like origin within the lithosphere (Moore 2014) or crystallization in the sublithospheric mantle (Smith et al. 2016), particular emphasis was placed on evaluating the presence or absence of inclusions indicative of a superdeep origin. A second goal of the study was to employ lithospheric inclusions in diamonds from Karowe to establish the compositional characteristics, the thermal conditions, and the thickness of the lithospheric mantle at the time of diamond formation.

Geological framework

The geology of Botswana is mainly defined by the domains of the Kalahari Super-Craton, which include the Archean basement of the Kaapvaal and Zimbabwe cratons sutured by the Archean to Paleoproterozoic Limpopo Mobile Belt (Fig. 1). In the west, the Kalahari Super-Craton is bounded by the Paleoproterozoic Kheis and Magondi orogenic belts (Fig. 1). The Kaapvaal Craton nucleated first and stabilised between 3.7 Ga to 2.6 Ga (De Wit et al. 1992). The formation of the core of the Zimbabwe Craton and its crustal growth occurred between 3.5 Ga to 2.6 Ga (Horstwood et al. 1999; Rollinson and Whitehouse 2011). The collision of the Kaapvaal and Zimbabwe cratons at about 2.7 to 2.6 Ga resulted in the formation of the Limpopo Mobile Belt (Van Reenen et al. 1987). The western Kheis and Magondi mobile belts range between 1.8 to 2.0 Ga in age (Majaule et al. 2001; Treloar 1988).

The Orapa, Letlhakane, Damtshaa, and Karowe mines form part of the Orapa kimberlite cluster, located in north-east Botswana, along the western edge of the Zimbabwe Craton (Fig. 1). The lithospheric mantle beneath this region has been studied for the past three decades both through diamonds and their mineral inclusions and through mantle xenoliths collected from the Orapa, Letlhakane, and Damtshaa kimberlites (Shee and Gurney 1979; Gurney et al. 1984). Inclusion studies revealed that the diamond sources beneath Orapa, Letlhakane, and Damtshaa are compositionally distinct (Deines and Harris 2004; Deines et al. 2009). At Letlhakane and Damtshaa, peridotitic inclusions are more common compared to a predominately eclogitic diamond association at Orapa. Peridotitic diamond substrates in the lithospheric mantle beneath Orapa were investigated by Stachel et al. (2004b), who found that inclusions in diamond reflect mild metasomatic overprint through CHO fluids compared to the extensive metasomatic modification observed in peridotite xenoliths (Griffin et al. 2003). The authors attributed this difference to peridotitic diamond formation that predated major modification of the lithosphere during Proterozoic rifting and compression. Stiefenhofer et al. (1997) conducted a detailed study on mantle xenoliths from Letlhakane, located approximately 40km southeast of Orapa. With the Orapa and Letlhakane kimberlites having been emplaced into the Proterozoic Magondi Belt (Fig. 1), this study, together with the Re-Os dating presented by Carlson et al. (1999), has established that both Letlhakane and Orapa are underlain by lithospheric mantle that is chemically depleted, cold, and old. This indicates that in the Orapa area, the Magondi Belt is thrust over the western edge of the Zimbabwe Craton (Stiefenhofer et al. 1997).

Outside the Orapa kimberlite cluster, information about the lithospheric mantle of the Zimbabwe Craton is principally based on mantle xenoliths and inclusion-bearing diamonds from the Cambrian kimberlites at Murowa and Sese, located in the southern part of the craton. The present evidence indicates that the lithospheric mantle beneath the southern Zimbabwe Craton is exceptionally depleted with diamond substrates of harzburgitic-dunitic paragenesis (Smith et al. 2009). Similar strongly depleted harzburgitic diamond sources were also established for the River Ranch kimberlite, located in the Central Zone of the Limpopo Mobile Belt (Kopylova et al. 1997). The Zimbabwe Craton and parts of the Limpopo Mobile Belt are underlain by a thick (~225 to 250 km) mantle root, with lithosphere thickness increasing even further towards the south beneath the Kaapvaal Craton (~250 to 300 km; Fouch et al. 2004).

Samples and analytical techniques

A total of 120 inclusion-bearing diamonds was selected from run-of-mine production at the sorting office of Karowe Diamond Mine in Gaborone, Botswana. The collected diamonds range in size from about 2 to 3 mm (the equivalent to -7+5, -9+7, and -11+9 Diamond Trading Company sieve classes). The diamonds were visually inspected under a binocular microscope and fully documented for shape, colour and surface features, before being photographed. Subsequently, inclusions were extracted by crushing of the diamonds in a purpose-built steel cracker, mounted individually in epoxy and polished to a 0.25 µm finish. The inclusions measured between 60 µm and 500 µm in longest dimension. From the initial 120 diamonds, 171 mineral inclusions were successfully recovered and prepared from 107 diamonds. For the remaining 13 diamonds, inclusions were either not recovered or lost during preparation.

Major and minor element compositions of mineral inclusions were analysed using a JEOL 8900R electron probe micro-analyser (EPMA). All elements were measured with an accelerating voltage of 20 kV, beam current of 20 nA and ≤2 µm beam diameter. Peak count times were 15-30 seconds and combined background times were 30-60 seconds. Standards for the two light major elements Si (Kα) and Mg (Kα) were pyrope garnet, diopside or forsterite (Fo90.5), depending on the mineral analyzed. For the remaining elements, standards were albite (Na-Kα), pyrope garnet (Al-Kα), apatite (P-Kα), sanidine (K-Kα), labradorite (Ca-Kα), rutile (Ti-Kα), chromium oxide (Cr-Kα), spessartine (Mn-Kα), fayalite (Fe-Kα), nickel wire (Ni-Kα). The standards are described in more detail in Czas et al. (this volume; thier Table S1), with exception of Fo90.5, which is from a spinel peridotite mantle xenoliths collected at Harrat al Kishb, Saudi Arabia (McGuire et al. 1992). The CITZAF correction (Armstrong

1995) was utilized for data reduction. Three to five spots were analysed on each sample depending on the size of the mineral grain. After assessing homogeneity, the oxide concentrations measured were then averaged for individual grains. The resulting detection limits typically are ≤0.02 wt% oxide.

Rare earth element (REE) and trace element concentrations for selected garnet and clinopyroxene inclusions were measured using a Resonetics M-50 193 nm excimer laser coupled with a Thermo Element XR 2 sector-field inductively coupled plasma mass spectrometer (LA-ICP-MS). Grains were ablated with a spot size of 50 or 75 μm at a laser frequency of 10 Hz and energy density of ~4 J/cm^2. For each sample two or three spots were analyzed and an average of 100 sweeps through the mass spectrum were made for each analysis. Measurement time comprised of 40 seconds background collection followed by 60 seconds sample ablation. The ICP-MS was operated at low mass resolution mode ($M/\Delta M$=ca. 300). The ThO/Th signal was monitored to ensure that oxide production remained below 0.5 %. Calibration of relative element sensitivities was performed using the NIST SRM 612 glass reference material and ^{43}Ca was employed as an internal standard to normalize the signal intensities. Data processing was performed offline using Iolite v3 (Paton et al. 2011). Detection limits are ≤30 ppb for REE, Nb, Zr, Y, Sr, and ~1 ppm for Ti and Ni.

Results

Most of the 107 diamonds contained a single mineral inclusion, commonly olivine (n=23; Table S1 in Electronic Supplementary Material A [ESM A]). Twenty-three diamonds hosted two-phase assemblages and one diamond a three-phase assemblage (Table S1 in ESM A). Inclusions were subdivided into the peridotitic (lherzolitic and harzburgitic), eclogitic, and websteritic suites based on mineralogy and major element composition (Grütter et al. 2004; Gurney et al. 1984; Meyer 1987.

Major element compositions of inclusions and paragenetic associations

Eclogitic suite

The 33 recovered eclogitic garnets can be divided into two groups on the basis of their CaO contents (Grütter et al. 2004): low-Ca (CaO <6 wt%; n=11) and high-Ca (CaO ≥6 wt%; n=22). As observed by Stachel and Harris (2008), there is a crude positive correlation between Na and Ca content (Table S1 in Electronic Supplementary Material B [ESM B]), both generally increasing from low- to high-Ca garnets and with the most Na_2O-rich garnet (0.54 wt%, diamond KW79) also having the highest CaO concentration (16.1 wt%). A similar crude positive correlation with Ca content exists for Ti, with the exception of unusually high TiO_2 (1.7 wt%) being observed in two garnets with intermediate CaO content (10.1 wt%) from diamond KW56. The two Ti-rich garnets show unusually low Al_2O_3 contents (average 19.9 wt%), with the typically six-fold coordinated cations Ti, Al, and Cr summing to 3.77 ([O]=24). As there is no excess of Si over the available tetrahedral sites in these garnets, this apparent deficiency can only be compensated through the presence of ferric iron (Canil and O'Neill 1996). In diamond KW36, a single garnet was associated with a deep blue kyanite (Table S1 in ESM B) and contained 7.0 wt% CaO, which is too low for derivation from typical grospydite (Sobolev et al. 1968). The three (low-Ca) garnets with the highest Mg# [~70; molar 100×Mg/(Mg+Fe)] also have elevated Cr_2O_3 contents (ranging from 0.52-0.80 wt%). These characteristics indicate an affinity to the websteritic inclusion suite (Deines et al.

1993) but fall in a compositional range where a clear distinction between low-Ca eclogitic and websteritic garnets is not possible (Stachel and Harris 2008).

The 40 analysed eclogitic clinopyroxene inclusions range in composition from augites (n=16) to omphacites [n=24; jadeite component calculated as 100×2Na/(2Na+Ca+Mg+Fe); Morimoto 1988]. The augites are unusual among eclogitic clinopyroxene inclusions worldwide with Cr_2O_3 contents extending to high values (average 0.15 wt%, max 0.27 wt%), high NiO (average 0.10 wt%), high MgO (average 19.8 wt%), and low jadeite contents (14.2-16.3 mol%) plus very low CaO (average 10.3, minimum 9.3 wt%). Their extremely low molar Ca# [100×Ca/(Ca+Mg+Fe)] of 23.3 (range 21.4-24.9) is unique among eclogitic inclusions worldwide, with the exception of inclusions from Letlhakane in the same kimberlite cluster (Deines and Harris 2004). For omphacites (25.8-48.2 mol% jadeite) there is a crude negative correlation between Mg# and Ti content. The two omphacites with the highest jadeite content (from diamond KW66) have an unusually high Mg# (91.4-91.7). With increasing Al content, Karowe omphacites deviate from the near 1:1 correlation between Al and Na cation content shown by eclogitic clinopyroxene inclusions worldwide towards excess Al (Fig. S1 in ESM A), suggestive of an additional, higher than normal Tschermaks component (Stachel and Harris 2008). Seven omphacites coexist with either low-Ca garnets (n=3 from one diamond) or high-Ca garnets (n=4 from two diamonds) garnets. For this sample set, clinopyroxenes associated with low-Ca garnet, compared to those occurring with high-Ca garnet, have a higher Mg# (average of 77.8 versus 71.7), Cr_2O_3 content (0.10 versus 0.04 wt%) and K_2O abundance (0.16 versus 0.06 wt%) at decreased CaO contents (12.2 versus 14.7).

Four SiO_2 (99.5-100.4 wt%) inclusions were recovered from four diamonds and are assumed to represent primary coesite. Of these, three co-exist with (1) a pair of low-Ca eclogitic garnets, (2) an omphacitic clinopyroxene, and (3) a low-Ni sulphide (monosulphide solid solution) inclusion, consistent with an eclogitic association. The fourth SiO_2 inclusion coexists with olivine (KW32e). Coesite may occur in peridotitic assemblages as a consequence of intense source carbonation (Wyllie and Huang 1976). As previously observed for inclusions in diamonds from the Renard Mine (Superior Craton; Hunt et al. 2012), the disequilibrium assemblage olivine + coesite requires continued diamond growth during progressive source carbonation, with the olivine inclusion representing an earlier growth stage. Two colourless and one deep blue kyanites inclusions were recovered. The latter coexisted with an orange garnet (KW36a; Table S1 in ESM B) and has elevated levels of TiO_2 (0.31 wt%), Cr_2O_3 (0.17 wt%), FeO (0.34 wt%), and MgO (0.18 wt%) compared to the two colourless kyanites that are ~99.8 % pure (Table S1 in ESM B).

Sulphide

Eighteen sulphide inclusions (12 single crystals and 6 polyphase grains; Table S2 in ESM B) are considered eclogitic. From the polyphase inclusions, five consist of two-phase and one of a three-phase assemblage. Inclusions were assigned an eclogitic paragenesis on the basis of co-existing eclogitic clinopyroxenes (n=2) and coesite (n=1) or <12 wt% Ni (Bulanova et al. 1996). A total of 25 sulphide phases were identified and plotted in a Fe-Ni- S quadrilateral diagram (Fig. S2 in ESM A). These include 12 occurrences of monosulphide solid solution (mss), of which 10 are Ni-poor (<10 wt%) and have a molar Ni/Fe ratio <0.2. Two are associated with separate chalcopyrite phases. Two remaining mss are Ni-rich (13.9-16.1 wt%), exceeding the cut-off value for typical eclogitic sulphides. Both are, however, still considered eclogitic on the basis of coexisting clinopyroxene inclusions (omphacite and low-Cr augite). The mss occurring with low-Cr augite additionally coexists with pentlandite containing 16.1 wt% Ni. Furthermore, the mss and pentlandite inclusions have detectable Cr contents (0.33 wt% and 0.29 wt%, respectively). Without the coexisting low-Cr augite inclusion, these two sulphides would have been assigned a peridotitic paragenesis (Stachel and Harris 2008), their compositions clearly reflect a chemically more depleted substrate than commonly observed for eclogitic inclusions. From the six low-Ni (<0.70 wt%) pyrrhotites, one coexisted with pyrite, one with a pyrite-chalcopyrite assemblage and one with pentlandite. This pentlandite is distinct with an elevated Co content (1.48 wt%) compared to all other eclogitic sulphide inclusions (<0.9 wt%). The remaining three inclusions mainly consist of pyrrhotite, with homogenous compositions. The Cu concentrations in chalcopyrite (n=3) range from 26.5 to 27.3 wt%.

Peridotitic suite

Of the nine peridotitic garnets recovered, eight are harzburgitic and one is lherzolitic (Fig. 2). Cr_2O_3 contents range from intermediate (5.7 wt%) to very high (14.7 wt%) and exceed the highest Cr_2O_3 concentrations previously recorded for a garnet inclusion from the Orapa kimberlite cluster (13.8 wt %; Deines and Harris 2004). Four garnets classify as low-Ca (CaO <1.8 wt%), indicative of derivation from extremely depleted, potentially dunitic sources (Grütter et al. 1999). Two of the harzburgitic and the one lherzolitic garnet record unusually high TiO_2 contents (0.19-0.24 wt%).

Thirty eight olivine inclusions have a narrow range in Mg# from 92.3 to 94.2 (Fig. 3), with a mean and median of 93.1. On the basis of coexisting garnets, six olivines can be assigned to the harzburgitic paragenesis with a Mg# mean (93.3) and median (93.1), similar to the remaining unassigned olivines, suggesting that all olivines may be harzburgitic. Karowe olivines fall into the normal ranges established for inclusions worldwide with the exception of three with unusual compositions: (1) two olivines have unusually low NiO (0.25 wt%; Fig. 3). One (KW31d) coexists with harzburgitic garnet and orthopyroxene and the other (KW32b) with coesite. (2) A single olivine in diamond KW111 has very high Cr_2O_3 (0.19 wt%), a feature that has been related to low Cr^{3+}/Cr^{2+} in the growth environment associated with unusually reducing conditions (Li et al. 1995; Bell et al. 2014).

Six orthopyroxene inclusions have a narrow range in Mg# (93.6-94.5; mean and median of 94.0) and show high CaO contents (0.31-0.62 wt% CaO) relative to the more common Ca-depleted harzburgitic orthopyroxenes (CaO ≤0.16 wt%; Stachel and Harris 2008). They fall into a compositional range where harzburgitic and lherzolitic enstatites overlap; based on coexisting garnets, one inclusion is harzburgitic (KW31) and one lherzolitic (KW49). The lone recovered diopside inclusion recovered has a Mg# of 93.1, similar to the median value (92.9) for lherzolitic clinopyroxene inclusions worldwide but is unusually low in Al_2O_3 (0.67 wt%), Cr_2O_3 (0.55 wt%) and Na_2O (0.29 wt%) content (Fig. S1 in ESM A). Eleven Mg-chromites recovered show compositions typical for inclusions in diamond, with high Cr# [85.6-93.3; 100×Cr/(Cr+Al)] and generally low TiO_2 contents (0.06-0.40 wt%), with a single exception (KW5;1.1 wt% TiO_2).

Sulphide

Four sulphide inclusions were classified as peridotitic. Of these, two are from a single diamond (KW101) where they co-existed with olivine, the other two are lone inclusions (Fig.S2 in ESM A). The two sulphides occurring with olivine are mss and have the elevated Cr contents (0.43 wt%) typically associated with a peridotitic paragenesis (Stachel and Harris 2008). The mss with the lower Ni content (16.3 wt%) shows exsolution of pentlandite around the edges and includes a platinum nugget (1µm diameter; detected by EDS). Of the two remaining sulphides, one is mainly composed of pentlandite (36.1 wt% Ni) and the other consists of pentlandite with a contact phase of Ni-Fe alloy (68.0 wt % Ni, 27.6 wt% Fe and 1.50 wt% Co) approximating the chemical composition of awaruite (Ni_2Fe to Ni_3Fe). The whole inclusion measured 120µm in diameter.

Websteritic suite

A single orthopyroxene inclusion (KW109b, Table S1 in ESM B) shows an exceptionally low Mg# (56.7), very high CaO (1.43 wt%), and elevated P_2O_5 (0.05 wt%; detection limit =0.02 wt%) and TiO_2 (0.21 wt%) concentrations. The inclusion falls far below the lower cut-off for peridotitic orthopyroxene inclusions at Mg# ~86 (Stachel and Harris 2008) and consequently is assigned to the websteritic suite.

Sublithospheric inclusions

Three "eclogitic" garnets recovered from two diamonds (KW50 and 57, Table S1 in ESM B) exhibit a variable majorite component. Based on 24 oxygens per formula unit, the single low-Ca eclogitic garnet contains 6.46 Si cations and has the high concentrations of TiO_2 (1.4 wt%) and Na_2O (0.77 wt%) often seen among majoritic garnets. The two high-Ca (9.3 wt% CaO) eclogitic garnets have a Si cation content of 6.12, which is only marginally elevated, but these garnets also contain high TiO_2 (1.0 wt%) and Na_2O (0.51 and 0.55 wt%). Their Mg# (42.6-42.8) is unusually low for garnets with a majorite component.

REE and trace element compositions of the inclusions

Eclogitic suite

For the eclogitic inclusion suite, trace element concentrations were determined on 13 garnets (12 diamonds; Fig. 4) and 13 clinopyroxenes (nine diamonds; Fig. S3). Three low-Ca garnets exhibit steep positive slopes within the $LREE_N$ that become less steep within the $MREE_N$-

$\mathrm{HREE_N}$, rising from ~0.1-0.2 times chondritic abundance for La to about 20-40 times chondritic level for Lu (Fig. 4a). The $\mathrm{REE_N}$ patterns for six high-Ca garnets also show steep positive slopes within the LREE but become flat from MREE to HREE at about 10 to 40 times chondritic abundance (Fig. 4a). The same distinction in $\mathrm{MREE_N}$-$\mathrm{HREE_N}$ slopes for low and high-Ca garnets was previously made by Beard et al. (1996) for eclogite xenoliths from the Mir kimberlite (Siberia). The remaining four high-Ca garnets (with the two garnets from KW81 being indistinguishable; Fig. 4b) have very unusual, flat $\mathrm{REE_N}$ patterns at about 2 to 20 times chondritic abundance. Mild positive Eu anomalies [geometric Eu/Eu* of 1.21-1.26; defined as $\mathrm{Eu_N/SQRT(Sm_N \times Gd_N)}$] are seen in high-Ca garnets KW79 (positive $\mathrm{LREE_N}$ slope and flat $\mathrm{MREE_N}$-$\mathrm{HREE_N}$), KW81a and b (flat $\mathrm{REE_N}$). Similar $\mathrm{REE_N}$ patterns are documented for some eclogitic garnet inclusions from the Premier (Cullinan) Mine (Viljoen et al. 2010). From the 13 $\mathrm{REE_N}$ patterns for clinopyroxenes, six omphacites and three low-Cr augites are characterized by a mild positive slope within the $\mathrm{LREE_N}$ and a steady decline within $\mathrm{MREE_N}$-$\mathrm{HREE_N}$ from Nd at 2-10 and Lu 0.2-3 chondritic abundance (Fig. S3a in ESM A). Of the remaining omphacitic clinopyroxenes, three have humped patterns, i.e. they show a more pronounced peak in the $\mathrm{LREE_N}$ at about 20-90 times chondritic abundances followed by steep negative slopes in $\mathrm{MREE_N}$-$\mathrm{HREE_N}$ (Fig. S3b in ESM A). The last omphacite (KW68b) shows the mild positive slope within the $\mathrm{LREE_N}$, as characteristic for the first group, followed by steeply declining $\mathrm{MREE_N}$-$\mathrm{HREE_N}$ like the second group (Fig. S3b). It is the only clinopyroxene to show a strong positive Eu anomaly (Eu/Eu*=1.51). Mild positive Eu anomalies (Eu/Eu*=1.21) are seen for the two omphacite inclusions from diamond KW65 (showing the mildly sloping $\mathrm{REE_N}$ patterns of the first group and coexisting with high-Ca garnet with Eu/Eu* of 1.15).

Eclogitic bulk rock $\mathrm{REE_N}$ patterns are calculated for five non-touching pairs of garnet and clinopyroxene (assuming a 1:1 modal abundance ratio; Table S3 in ESM B). Of the three bulk rocks calculated involving high-Ca garnets, two have $\mathrm{REE_N}$ patterns subparallel to N-MORB with overall lower REE concentrations and more pronounced depletions in LREE (Fig. S4a in ESM A). The third sample (KW56) shows similar HREE concentrations but is distinctly enriched in LREE (to concentrations greater than N-MORB; Fig.S4a). The two pairs involving low-Ca garnets exhibit a gradual increase from $LREE_N$ to $HREE_N$ with N-MORB like HREE (Fig S4b in ESM A). The overall REE depletion and, in two cases, low LREE/HREE for bulk rocks involving high-Ca garnets are all similar to the observations of Beard et al. (1996) for high-Ca eclogite xenoliths. The negative $LREE_N$-$HREE_N$ slope for the KW56 bulk rock suggests that at Karowe the eclogitic substrates for the high-Ca group were locally affected by cumulate enriched protoliths with metasomatically added LREE.

Peridotitic Suite

Six harzburgitic and one lherzolitic garnet were analysed for trace element contents. Three harzburgitic garnets show typical sinusoidal REE_N patterns peaking in the LREE (Ce-Nd), a low at Dy-Er and steep positive slopes towards Lu (Fig. S5a in ESM A). A fourth sinusoidal pattern is unusual in peaking only in the MREE (at ~10 chondritic abundance for Eu) and having overall super-chondritic MREE and HREE (Fig. S5a). The remaining two harzburgitic garnets have comparatively flat, slightly U-shaped REE_N patterns in the range of 0.3-4 times chondritic abundance (Fig. S5b in ESM A). The single lherzolitic garnet has a normal REE_N pattern with LREE depleted and flat $MREE_N$-$HREE_N$ at about 4 times chondritic abundance (Fig. S5b).

Sublithospheric inclusions

The two analyzed majoritic garnets show opposite REE_N patterns (Fig. 5): the low-Ca majorite displays a steep negative slope from $LREE_N$ at ~100 times to $HREE_N$ at ~1 times chondritic abundance. The high-Ca majoritic garnet rises from chondritic $LREE_N$ abundance to 300 times chondritic $HREE_N$.

Geothermobarometry

In ten diamonds two or more mineral inclusion species coexisted that are suitable for the calculation of equilibrium temperatures and/or pressures (Table S2 in ESM A). Five non-touching pairs of eclogitic garnet and clinopyroxene yield equilibrium temperatures of 1260-1480 °C, using the Fe-Mg exchange thermometer of Krogh (1988) at a pre-set pressure of 5 GPa. Two pairs involving low-Ca garnets give lower temperatures (1260-1270 °C), compared to three involving high-Ca garnets (1420-1480 °C; Table S2 in ESM A). A similar dichotomy is not observed for Orapa, where pairs of clinopyroxene and low-Ca (n=3) or high-Ca garnets (n=6) yield average equilibration temperatures of 1150 and 1160 °C, respectively (calculated from the dataset of Deines et al. 1993 and Gurney et al. 1984). For Letlhakane, only one pair of clinopyroxene and low-Ca garnet was analysed (yielding 1320 °C), the eight pairs involving high-Ca garnets yield an average of 1210 °C (calculated from the data set of Deines and Harris, 2004). A separation into cool (shallow) low-Ca and hot (deep) high-Ca eclogites, therefore, is not a general feature of the lithospheric mantle beneath the Orapa kimberlite cluster.

For the peridotitic suite, one touching (KW86) and three non-touching garnet-olivine pairs (KW31, 69 and 74) give a temperature range of 900-1245 °C (Table S2 in ESM A), based on the garnet-olivine thermometer of O'Neill and Wood (1979; calculated at 5 GPa). Diamond KW31, in addition to garnet and olivine, also hosted a non-touching orthopyroxene; application of the garnet-orthopyroxene Fe-Mg exchange thermometer of Harley (1984) yielded a temperature of 1180 °C at pre-set pressure of 5 GPa (Table S2 in ESM A), which is within error of the 1245 °C estimate obtained with the olivine-garnet thermometer (O'Neill and Wood 1979). This suggests that olivine, orthopyroxene and garnet in this diamond likely are in equilibrium. Simultaneous estimation of pressure and temperature using garnet-orthopyroxene geothermobarometry (Brey and Köhler 1990; Harley 1984) yields 5.2 GPa and 1200 °C as a condition of inclusion entrapment. Application of the same geothermobarometer combination to a second non-touching garnet-orthopyroxene pair in diamond KW49 gives 4.1 GPa at 950 °C (Table S2 in ESM A), resulting in the two samples plotting along a 39-40 mW/m^2 (Hasterok and Chapman 2011) model geotherm (Fig. S6 in ESM A). This result is in very good agreement with the 40 mW/m^2 paleogeotherm derived by Stiefenhofer et al. (1997) for peridotite xenoliths from the nearby Cretaceous Letlhakane kimberlite. The single lherzolitic clinopyroxene inclusion (KW 93) could not be used for geothermobarometric calculations as it fails the compositional filters of Grütter (2009).

Based on the Ca-in-opx thermometer (Brey and Köhler 1990), the single websteritic inclusions last equilibrated at 1380 °C. Such a high temperature is not typically associated with diamond formation along steady state cratonic geotherms (Stachel and Luth 2015) but suggests either association with a thermal perturbation (magmatic intrusion) within the lithosphere or derivation from below the lithospheric mantle. Given that this temperature falls within the range observed for eclogitic (non-majoritic) garnet and clinopyroxene pairs from Karowe (see above), a lithospheric origin appears plausible. Pressure determinations for the three majoritic garnet inclusions from Karowe using the barometer of Beyer and Frost (2017) range between 11 and 14 GPa, clearly implying a sublithospheric origin (Fig. 6).

Discussion

Of the 107 inclusion-bearing diamonds studied here, 53 % are eclogitic, 44 % peridotitic, 2 % sublithospheric, and 1 % websteritic. This predominantly eclogitic diamond production at Karowe is similar to the Orapa mine but unlike the predominantly peridotitic productions of the adjacent Letlhakane and Damtshaa mines.

Origin and evolution of eclogitic and websteritic diamond substrates

Eclogitic garnet and clinopyroxene inclusions from Karowe are compositionally variable but for the most part, compare well to previous studies on inclusions in diamonds from the Orapa kimberlite cluster. A comparison of Karowe garnet compositions with other garnets inclusions from the Orapa cluster is shown in Figure S7 in ESM A. A websteritic inclusion suite was first recognized in diamonds from the Orapa kimberlite (Gurney et al. 1984) and documents the presence of an unusually wide spectrum of “mafic” diamond substrates in the local lithospheric mantle. This is also evident from the compositions of a large suite of eclogite and pyroxenite xenoliths from the Orapa (Aulbach et al. 2017). In Karowe, the presence of orthopyroxene-bearing (websteritic) substrates is evidenced by a single enstatite inclusion with low Mg# (57). Possible saturation in orthopyroxene may also be indicated by Ca# as low as 21.5 in augite inclusions with elevated Cr, Ni, and Mg contents. Mineralogical variability in the eclogitic substrates is also highlighted by the occasional presence of kyanite and coesite inclusions. Kyanite occurs in Group I diamondiferous eclogites from Orapa (Shee and Gurney 1979) and was recently described in Group II diamond-free eclogites by Aulbach et al. (2017). It is a characteristic phase of aluminous eclogites in general (Spetsius 2004; Shu et al.2016).

The REE characteristics (bulk rock $LREE_N/HREE_N$ generally <1; presence of positive Eu anomalies in some high-Ca garnets and coexisting clinopyroxenes) are consistent with a derivation of Karowe low- and high-Ca eclogitic diamond substrates from subducted protoliths. Moderate positive Eu anomalies in two of the calculated bulk rocks involving high-Ca garnets (Fig. S8 in ESM A) suggest cumulate enriched protoliths for these samples (e.g., Aulbach and Viljoen 2015). The absence of distinct positive Sr anomalies for the same calculated bulk rocks (Fig. S8), however, indicates decoupling of Sr and Eu/Eu*. A decoupling of Sr content and Eu/Eu* is also observed for garnet inclusions in diamonds world-wide and was related to Sr depletion during secondary partial melting events (Stachel et al. 2015). Positive Sr anomalies without paired Eu anomalies in the two calculated low-Ca group bulk rocks (Fig. S8) again show decoupling of Sr content and Eu/Eu*. Positive slopes from MREE to HREE (Yb_N/Gd_N=2.2-3.3) indicate that the protoliths of the low-Ca eclogitic diamond substrates likely experienced partial melting and associated depletion in LREE (Fig. S-4), followed by metasomatic re-enrichment in Sr (Aulbach et al. 2017). Estimated bulk rock Mg# of 61-72 are on the high side of average present-day N-MORB (~60; Floyd 1991) and could be inherited from gabbroic protoliths (Aulbach and Jacob 2016) or again reflect a secondary melting extraction event.

Combining the observed variability in the major element compositions of garnet and clinopyroxene inclusions with the range of bulk rock REE_N patterns indicates that a large cross section of oceanic crust (not necessarily related to a single subduction event) was sampled. Beard et al. (1996) suggested an origin of high-Ca eclogites as cumulate-enriched rocks of the deeper oceanic crust (causing overall REE depletion increasing towards the LREE) and low-Ca eclogites as upper oceanic crust (with relatively unfractionated REE). At Karowe, the presence of positive Eu anomalies only in high-Ca garnets and associated clinopyroxenes is consistent with this model. Subsequent modification during partial melting in the garnet stability field (LREE loss; Foley et al. 2002; Jacob 2004), metasomatic modification (LREE addition; Ireland et al. 1994) and interaction with mantle peridotite (adding Cr and Mg; Smart et al. 2009) may all have acted to increase the compositional variance further and, in combination, cause compositionally diverse eclogitic to pyroxenitic diamond substrates beneath Karowe.

Peridotitic diamond substrates in the lithospheric mantle beneath Karowe

Peridotitic olivine inclusions in Karowe diamonds have high Mg# with a mean and median of 93.1, comparable to olivine inclusions from elsewhere in the Orapa cluster (e.g., Deines et al. 2009) and harzburgitic olivine inclusions worldwide (mean: 93.2; Stachel and Harris 2008). Such high forsterite contents imply the presence of peridotitic mantle sources that experienced primary melt extraction approaching and exceeding the exhaustion of orthopyroxene (Bernstein et al. 2007). Two Karowe olivines with normal Mg# have unusually low NiO contents (mean of 0.26 wt% as opposed to 0.36 wt% worldwide; Fig. 3). Unusually low Ni contents were shown to occur in olivine inclusions that originated as ringwoodite in equilibrium with ferropericlase in the lower transition zone (Brey et al. 2004). However, the two low-Ni olivines from Karowe have low P_2O_5, Cr_2O_3 and Na_2O, inconsistent with a superdeep origin, and in one case (KW31) occur in apparent equilibrium with normal lithospheric inclusions (harzburgitic garnet and orthopyroxene).

Peridotitic garnet inclusions from Karowe are dominantly (~90 %) harzburgitic and almost half have CaO contents < 1.8 wt%, i.e. likely originating from primary residues that were molten beyond the point of orthopyroxene exhaustion (Grütter et al. 1999). One of the low-Ca garnets has a very high Cr_2O_3 content (14.7 wt%) that implies that at the time of diamond formation highly depleted cratonic lithosphere extended down to at least 220 km depth (equivalent to 7 GPa pressure; Fig. 2; Grütter et al. 2006) beneath Karowe. These observations establish that the lithospheric mantle beneath Karowe, at least at the time of peridotitic diamond formation, was strongly depleted in easily fusible components and very thick, similar to the southern part of the Zimbabwe Craton (Smith et al. 2009). REE_N patterns for harzburgitic garnets (sinusoidal to slightly U-shaped) and the one lherzolitic garnet (normal REE_N) are very distinct and imply different styles of metasomatic re-enrichment: fluid metasomatism for the harzburgitic and melt metasomatism for the lherzolitic substrates (Stachel et al. 2004a). The Y and Zr concentrations of these garnets (Fig. S9 in ESM A) are consistent with this conclusion: all but one harzburgitic garnet plot in the depleted field but clearly define a trend that leads into the field for low temperature, fluid-style metasomatism. Whereas the single lherzolitic garnet documents a much higher Y/Zr ratio, consistent with melt metasomatism. Very similar garnet REE_N patterns to those observed at Karowe (sinusoidal and slightly U-shaped for harzburgitic and normal for the one lherzolitic garnet) and metasomatic styles (fluid metasomatism for harzburgitic and melt metasomatism for lherzolitic garnets) were also documented for peridotitic garnet inclusions in diamonds from Orapa (Fig. S9; Stachel et al. 2004b).

The presence of a Ni-Fe alloy inclusion (intergrown with pentlandite) indicates that, at least locally, fO_2 conditions as reducing as the iron-wüstite buffer occurred in the peridotitic diamond substrates. Generally, such reducing conditions are not observed within lithospheric mantle, even for cratons of similar depth extent (Stagno et al. 2013), and hence are interpreted as a localized environment rather than widespread metal saturation in the deep mantle lithosphere below the Zimbabwe Craton.

Sublithospheric substrates

Pressure determinations for the three majoritic garnet inclusions from two Karowe diamonds place their origin in the deep asthenosphere and uppermost transition zone (between 330 and 420 km depth; Fig. 6b). Based on their low-Cr character (cut-off at Cr_2O_3 <1 wt%; Schulze 2003), the majoritic garnets all derive from eclogitic substrates. Kiseeva et al. (2013) reported that despite their overall eclogitic mineral compositions, such majoritic garnets can follow (1) a substitution mechanism ($2Al^{3+}=Si^{4+}+M^{2+}$) that is characteristic for peridotitic (and pyroxenitic) substrates or (2) a substitution mechanism (eclogitic trend) accommodating the jadeite component of omphacitic clinopyroxene ($M^{2+}+Al^{3+}=Na^{+}+Si^{4+}$) . The first substitution (pyroxenitic trend) is interpreted to reflect sublithospheric diamond formation through interaction of slab-derived magnesio-carbonatitic melt and adjacent pyrolytic mantle (Kiseeva et al. 2016, Walter et al. 2008). At Karowe, the low-Ca majoritic garnet in diamond KW50 shows an excess in Mg+Ca+Fe+Mn over the number of available X-sites in garnet and thus falls onto the pyroxenitic trend, while the two high-Ca majoritic garnets in KW57 fall onto the Na-majorite trend (Harte 2010; Kiseeva et al. 2013). The low-Ca majoritic garnet has an elevated Cr_2O_3 content (0.18 wt%) and Mg# (66.2), consistent with the pyroxenitic connection suggested by Kiseeva et al. (2013 and 2015), whilst the two high-Ca garnets contain Cr below the limit of detection and have low Mg# (average of 42.7), indicative of a typical eclogitic bulk rock composition (Harte 2010). This clear separation into two modes of majorite formation is reflected in highly distinct REE_N patterns for low- and high-Ca majoritic garnets (Fig.5). The low-Ca garnet exhibits a melt-like pattern characterized by strong LREE enrichment and a steeply negative slope from $LREE_N$ to $HREE_N$. Based on the majorite-melt partition coefficients of Yurimoto and Ohtani (1992), the REE_N pattern of a calculated melt in equilibrium with the low-Ca garnet would show a steep decline from 540 times chondritic La to chondritic Yb abundance. The high-Ca garnet has the reverse pattern with a steep positive $LREE_N$-$HREE_N$ slope. Although more enriched in HREE, the high-Ca garnet REE_N pattern is similar to those displayed by eclogitic majoritic garnets from Monastery (Moore et al. 1991) and Jagersfontein (Tappert et al. 2005; Fig.5). The strong HREE enrichment would be consistent with the high-Ca garnet crystallizing in a residuum that yielded a melt similar to that forming the low-Ca majoritic garnets.

Karowe Mine produces large to extremely large gem-quality diamonds that are nitrogen “free” Type IIa or Type IaB containing low contents of completely aggregated nitrogen (D’Haenens-Johansson et al. 2017). Smith et al. (2016) studied large Type IIa diamonds from several sources and found that they exclusively contained inclusions of sublithospheric origin, including majoritic garnets. Inclusions of sublithospheric origin have not previously been reported in diamonds from the Orapa kimberlite cluster. The two majoritic garnet-bearing diamonds from Karowe reported here are not Type IIa but have very low to moderate nitrogen contents of highly aggregated nitrogen (30 and 250 at.ppm with 95 and 86 %B respectively). Nevertheless, their discovery shows that sublithospheric diamond sources were tapped by the Karowe kimberlite, an indication that the very large diamonds from this mine also formed at below the lithosphere, as observed elsewhere by Smith et al. (2016).

Conclusions

The major element composition of inclusions in Karowe diamonds establishes their derivation from four distinct mantle lithologies present below the western edge of Zimbabwe Craton. More than half of the diamond population is eclogitic (53 %), followed by peridotitic (44 %), sublithospheric (2 %) and websteritic (1 %). Overall, the composition of the eclogitic and peridotitic inclusions compares well with the results of previous studies conducted on other localities in the Orapa kimberlite cluster (on diamonds from Orapa, Damtshaa and Letlhakane). The eclogitic diamond substrates beneath Karowe are highly diverse, ranging from typical basaltic to cumulate-like protolith compositions. This variety is documented in the variance of calculated bulk rock Mg# (61-72) and the broad range in the jadeite component (14-48 mol%) in eclogitic clinopyroxenes as well as the presence of three kyanite inclusions. In combination with calculated bulk rock REE patterns, the variable inclusion chemistry documents derivation of eclogitic diamonds from a range of protoliths that represent both shallow and deep oceanic crust, in part modified by partial melting during subduction and subsequent metasomatism. About 40 % of eclogitic clinopyroxenes are augites with elevated contents of Cr, Ni and Mg at unusually low Ca contents, which may represent an association transitional to pyroxenites. A single websteritic orthopyroxene inclusion confirms the presence of pyroxenitic diamond substrates beneath Karowe that were also recognized at Orapa.

The peridotitic inclusion suite documents a predominance of typical, highly depleted diamond substrates of harzburgitic to dunitic paragenesis along the western margin of the Zimbabwe Craton. Very high Cr_2O_3 in one of the low-Ca peridotitic garnets is indicative of a depth extent of this highly depleted cratonic lithosphere to at least 220 km depth at the time of diamond formation.

The discovery of sublithospheric (eclogitic majoritic garnet) inclusions in Karowe diamonds sets this mine apart from other deposits in the Orapa kimberlite cluster and may provide a key link to the regular recovery of exceptionally large diamonds at Karowe. Low-Ca and high-Ca majoritic garnets follow two distinct trends of majoritic substitution (pyroxenitic and eclogitic trend, respectively). These distinct origins are consistent with their REE_N patterns being mirror images: (1) high LREE and low HREE for the low Ca-garnet, suggested to relate to melt-aided slab-pyrolite interaction and (2) low LREE and high HREE for the high-Ca garnet, which formed in substrates representing basaltic protoliths that lost a partial melt similar to that reflected in the low-Ca majorites.

Acknowledgments

Lucara Diamond Corporation is sincerely thanked for the provision of production diamonds for this study and JWH also extents gratitude to the Company for the hospitality and resources provided, which enabled the diamonds to be collected. John Gurney (Cape Town) is thanked for bringing the project to the Lucara board and getting us started. T.M. thanks Janina Czas and Nicole Meyer (University of Alberta) for comments, discussions and advice that helped to improve this manuscript. Thoughtful reviews by Sonja Aulbach (Frankfurt) and Ben Harte (Edinburgh) are gratefully acknowledged. Andrew J. Locock is thanked for his assistance and advice related to microprobe analyses. T.M. received a bursary from the Government of Botswana as part of Pre-University Academic Programmes under Botswana International University of Science and Technology (BIUST). T.S. acknowledges research funding through an NSERC Discovery grant and the Canada Research Chairs program.

References

Armstrong JT (1995) CITZAF-a package of correction programs for the quantitative electron microbeam X-ray of thick polished materials, thin-films, and particles. Microbeam Anal 4:177-200

Aulbach S, Jacob DE, Cartigny P, Stern RA, Simonetti SS, Wörner G, Viljoen KS (2017) Eclogite xenoliths from Orapa: Ocean crust recycling, mantle metasomatism and carbon cycling at the western Zimbabwe craton margin. Geochim Cosmochim Acta 213:574-592

Aulbach S, Viljoen KS (2015) Eclogite xenoliths from the Lace kimberlite, Kaapvaal Craton:From convecting mantle source to palaeo-ocean floor and back. Earth Planet Sci Lett 431:274-286

Aulbach S, Jacob DE (2016) Major-and trace-elements in cratonic eclogites and pyroxenites reveal heterogeneous sources and metamorphic processing of low-pressure protoliths. Lithos 262:586-605

Beard BL, Fraracci KN, Clayton RA, Mayeda TK, Snyder GA, Sobolev NV, Taylor LA (1996) Petrography and geochemistry of eclogites from the Mir kimberlite, Yakutia, Russia. Contrib Mineral and Petrol 125:293-310

Bell AS, Burger PV, Le L, Shearer CK, Papike JJ, Sutton SR, Newville M, Jones J (2014) XANES measurements of Cr valence in olivine and their applications to planetary basalts. Am Mineral 99(7):1404-1412

Bernstein S, Kelemen PB, Hanghøj K (2007) Consistent olivine Mg# in cratonic mantle reflects Archean mantle melting to the exhaustion of orthopyroxene. Geology 35(5):459-462

Beyer C, Frost DJ (2017) The depth of sub-lithospheric diamond formation and the redistribution of carbon in the deep mantle. Earth Planet Sci Lett 461:30-39

Brey GP, Köhler T (1990) Geothermobarometry in four-phase lherzolites II. New thermobarometers, and practical assessment of existing thermobarometers. J Petrol 31(6):1353-1378

Brey GP, Bulatov V, Girnis A, Harris JW, Stachel T (2004) Ferropericlase-a lower mantle phase in the upper mantle. Lithos 77:655-663

Bulanova GP, Griffin WL, Ryan CG, Shestakova OY, Barnes SJ (1996) Trace elements in sulfide inclusions from Yakutia diamonds. Contrib Mineral Petrol 124:111-125

Canil D, O'Neill HSC (1996) Distribution of ferric iron in some upper-mantle assemblages. J Petrol 37 (3):609-635

Carlson RW, Pearson DG, Boyd FR, Shirey SB, Irvine G, Menzies AH, Gurney JJ (1999) Re–Os systematics of lithospheric peridotites: implications for lithosphere formation and preservation. Proceedings 7th International Kimberlite Conference, Red Roof Design, Cape Town, pp 99-108

D'Haenens-Johansson UFS, Smith EM, Smit KV, Wang W, Moses TM (2017) The 812-carat pure Type IaB constellation diamond from Karowe- Part of an even larger rough? Extended Abstracts, 11th International Kimberlite Conference, Gaborone, Botswana. No. 11IKC-4611

De Wit MJ, de Ronde CE, Tredoux M, Roering C, Hart RJ, Armstrong RA, Green RW, Peberdy E, Hart RA (1992) Formation of an Archaean continent. Nature 357(6379):553-562

Deines P, Harris JW (2004) New insights into the occurrence of ^{13}C-depleted carbon in the mantle from two closely associated kimberlites: Letlhakane and Orapa, Botswana. Lithos 77:125-142

Deines P, Stachel T, Harris JW (2009) Systematic regional variations in diamond carbon isotopic composition and inclusion chemistry beneath the Orapa kimberlite cluster, in Botswana. Lithos 112:776-784

Deines P, Harris JW, Gurney JJ (1993) Depth-related carbon isotope and nitrogen concentration variability in the mantle below the Orapa kimberlite, Botswana, Africa. Geochim Cosmochim Acta 57(12):2781-2796

Floyd P (1991) Oceanic basalts. Springer (New York), pp 456

Foley S, Tiepolo M, Vannucci R (2002) Growth of early continental crust controlled by melting of amphibolite in subduction zones. Nature 417(6891):837-840

Fouch MJ, James DE, VanDecar JC, van der Lee S, Kaapvaal SG (2004) Mantle seismic structure beneath the Kaapvaal and Zimbabwe Cratons. South African J Geol 107(1-2):33-44

Griffin WL, O'Reilly SY, Natapov LM, Ryan CG (2003) The evolution of lithospheric mantle beneath the Kalahari Craton and its margins. Lithos 71:215-241

Grütter H, Latti D, Menzies A (2006) Cr-saturation arrays in concentrate garnet compositions from kimberlite and their use in mantle barometry. J Petrol 47:801-820

Grütter HS (2009) Pyroxene xenocryst geotherms: Techniques and application. Lithos 112(Supplement 2):1167-1178

Grütter HS, Apter DB, Kong J (1999) Crust–mantle coupling: evidence from mantle-derived xenocrystic garnets. In Gurney JJ, Gurney JL, Pasco MD, Richardson SH (Eds), The J.B Dawson Volume, Proceedings of the VIth International Kimberlite Conference, Red Roof Design, Cape Town, pp 307-313

Grütter HS, Gurney JJ, Menzies AH, Winter F (2004) An updated classification scheme for mantle-derived garnet, for use by diamond explorers. Lithos 77:841-857

Gurney JJ, Harris JW, Rickard RS (1984) Silicate and oxide inclusions in diamonds from the Orapa Mine, Botswana. Kimberlites II: the mantle and crust-mantle relationships. Elsevier, Amsterdam, pp 3-9

Harley SL (1984) An experimental study of the partitioning of Fe and Mg between garnet and orthopyroxene. Contrib Mineral Petrol 86:359-373

Harte B (2010) Diamond formation in the deep mantle: the record of mineral inclusions and their distribution in relation to mantle dehydration zones. Min Mag 74(2):189-215

Hasterok D, Chapman DS (2011) Heat production and geotherms for the continental lithosphere. Earth Planet Sci Lett 307:59-70

Horstwood MS, Nesbitt RW, Noble SR, Wilson JF (1999) U-Pb zircon evidence for an extensive early Archean craton in Zimbabwe: A reassessment of the timing of craton formation, stabilization, and growth. Geology 27(8):707-710

Hunt L, Stachel T, McCandless TE, Armstrong J, Muehlenbachs K (2012) Diamonds and their mineral inclusions from the Renard kimberlites in Quebec. Lithos 142:267-284

Ireland TR, Rudnick RL, Spetsius Z (1994) Trace elements in diamond inclusions from eclogites reveal link to Archean granites. Earth Planet Sci Lett 128:199-213

Jacob DE (2004) Nature and origin of eclogite xenoliths from kimberlites. Lithos 77:295-316

Key RM, Ayres N (2000) The 1998 edition of the national geological map of Botswana. J African Earth Sci 30(3):427-451

Kiseeva ES, Wood BJ, Ghosh S, Stachel T (2016) The pyroxenite-diamond connection. Geochem Perspectives Lett 2:1-9

Kiseeva ES, Yaxley GM, Stepanov AS, Tkalčić H, Litasov KD, Kamenetsky VS (2013) Metapyroxenite in the mantle transition zone revealed from majorite inclusions in diamonds. Geology 41:883-886

Kopylova MG, Gurney JJ, Daniels LR (1997) Mineral inclusions in diamonds from the River Ranch kimberlite, Zimbabwe. Contrib Mineral Petrol 129: 366-366

Krogh EJ (1988) The garnet-clinopyroxene Fe-Mg geothermometer-a reinterpretation of existing experimental data. Contrib Mineral Petrol 99:44-48

Li JP, O'Neill HSC, Seifert F (1995) Subsolidus phase relations in the system MgO-SiO_2-Gr-O in equilibrium with metallic Cr, and their significance for the petrochemistry of Chromium. J Petrol 36(1):107-132

Majaule T, Hanson RE, Key RM, Singletary SJ, Martin MW, Bowring SA (2001) The Magondi Belt in northeast Botswana: regional relations and new geochronological data from the Sua Pan area. J Afr Earth Sci 32(2):257-267

McDonough WF, Sun S (1995) The composition of the Earth. Chem Geol 120(3-4):223-253.

McGuire AV, Francis CA, Dyar MD (1992) Mineral standards for electron microprobe analyses of oxygen. Am Mineral 77:1087-1091

Meyer H (1987) Inclusions in diamond. In Nixon PH (ed) Mantle xenoliths, vol. John Wiley & Sons Ltd., Chichester, pp 501-522

Moore AE (2014) The origin of large irregular gem-quality type II diamonds and the rarity of blue type IIb varieties. South African J Geol 117:219-236

Moore RO, Gurney JJ, Griffin WL, Shimizu N (1991) Ultra-high pressure garnet inclusions in Monastery diamonds: trace element abundance patterns and conditions of origin. Eur J Mineral 3:213-230

Morimoto N (1988) Nomenclature of pyroxenes. Schweizerische Mineralogische und Petrographische Mitteilungen 68:95-111

O'Neill HSC, Wood BJ (1979) An experimental study of Fe-Mg partitioning between garnet and olivine and its calibration as a geothermometer. Contrib Mineral Petrol 70:59-70

Paton C, Hellstrom J, Paul B, Woodhead J, Hergt J (2011) Iolite: Freeware for the visualisation and processing of mass spectrometric data. J Anal At Spectrom 26:2508-2518

Rollinson HR, Whitehouse M (2011) The growth of the Zimbabwe Craton during the late Archaean: An ion microprobe U-Pb zircon study. J Geol Soc 168(4):941-952

Schulze DJ (2003) A classification scheme for mantle-derived garnets in kimberlite: a tool for investigating the mantle and exploring for diamonds. Lithos 71:195-213

Shee SR, Gurney JJ (1979) The Mineralogy of xenoliths from Orapa, Botswana. In: Boyd FR, Meyer HOA (eds) The mantle sample: inclusions in kimberlites and related rocks.

Proceedings of the Second International Kimberlite Conference, Am Geophys Union 2:37-49

Shu Q, Brey GP, Hoefer HE, Zhao Z, Pearson DG (2016) Kyanite/corundum eclogites from the Kaapvaal Craton: subducted troctolites and layered gabbros from the Mid-to Early Archean. Contrib Mineral and Petrol 171:11-34

Smart KA, Heaman LM, Chacko T, Simonetti A, Kopylova M, Mah D, Daniels D (2009) The origin of high-MgO diamond eclogites from the Jericho Kimberlite, Canada. Earth Planet Sci Lett 284(3-4):527-537

Smith CB, Pearson DG, Bulanova GP, Beard AD, Carlson RW, Wittig N, Sims K, Chimuka L, Muchemwa E (2009) Extremely depleted lithospheric mantle and diamonds beneath the southern Zimbabwe Craton. Lithos 112:1120-1132

Smith EM, Shirey SB, Nestola F, Bullock ES, Wang J, Richardson SH, Wang W (2016) Large gem diamonds from metallic liquid in Earth’s deep mantle. Science 354:1403-1405

Sobolev Jr NV, Kuznetsova IK, Zyuzin NI (1968) The petrology of grospydite xenoliths from the Zagadochnaya kimberlite pipe in Yakutia. J Petrol 9:253-280

Spetsius ZV (2004) Petrology of highly aluminous xenoliths from kimberlites of Yakutia. Lithos 77:525-538

Stachel T, Luth RW (2015) Diamond formation-Where, when and how? Lithos 220-223:200-220

Stachel T, Harris JW (2008) The origin of cratonic diamonds-constraints from mineral inclusions. Ore Geol Rev 34:5-32

Stachel. T, Harris. JW, Hunt. L, Muehlenbachs. K, Kobussen. A, EIMF (2015) Argyle diamonds- How subduction along the Kimberley Craton edge generated the world's biggest's diamond deposit. Soc Econ Geol, Spec Publ, 20

Stachel T, Aulbach S, Brey GP, Harris JW, Leost I, Tappert R, Viljoen KF (2004a) The trace element composition of silicate inclusions in diamonds: a review. Lithos 77:1-19

Stachel T, Viljoen KS, McDade P, Harris JW (2004b) Diamondiferous lithospheric roots along the western margin of the Kalahari Craton-the peridotitic inclusion suite in diamonds from Orapa and Jwaneng. Contrib Mineral Petrol 147:32-47

Stagno V, Ojwang DO, McCammon CA, Frost DJ (2013) The oxidation state of the mantle and the extraction of carbon from Earth's interior. Nature 493:84-88

Stiefenhofer J, Viljoen KS, Marsh JS (1997) Petrology and geochemistry of peridotite xenoliths from the Letlhakane kimberlites, Botswana. Contrib Mineral Petrol 127(1-2):147-158

Tappert R, Stachel T, Harris JW, Muehlenbachs K, Ludwig T, Brey GP (2005) Subducting oceanic crust: the source of deep diamonds. Geology 33:565-568

Treloar PJ (1988) The geological evolution of the Magondi mobile belt, Zimbabwe. Precambrian Res 38(1):55-73

Van Reenen DD, Barton JM, Roering C, Smith CA, Van Schalkwyk JF (1987) Deep crystal response to continental collision: The Limpopo belt of southern Africa. Geology 15(1):11-14

Viljoen F, Dobbe R, Harris J, Smit B (2010) Trace element chemistry of mineral inclusions in eclogitic diamonds from the Premier (Cullinan) and Finsch kimberlites, South Africa: implications for the evolution of their mantle source. Lithos 118:156-168

Walter MJ, Bulanova GP, Armstrong LS, Keshav S, Blundy JD, Gudfinnsson G, Lord OT, Lennie AR, Clark SM, Smith CB (2008) Primary carbonatite melt from deeply subducted oceanic crust. Nature 454(7204):622-630

Wyllie PJ, Huang W (1976) Carbonation and melting reactions in the system CaO-MgO-SiO_2-CO_2 at mantle pressures with geophysical and petrological applications. Contrib Mineral Petrol 54:79-107

Yurimoto H, Ohtani E (1992) Element partitioning between majorite and liquid: a secondary ion mass spectrometric study. Geophys Res Lett 19(1):17-20

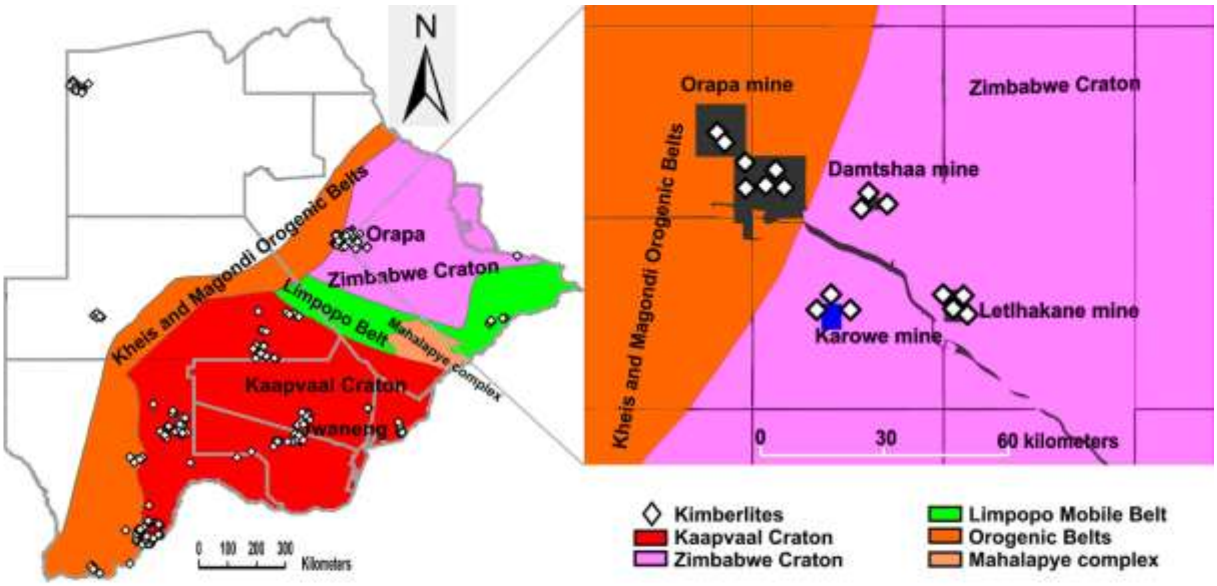

Fig. 1 Setting of the Karowe Mine in the geology of Botswana. Map modified after Key and Ayres (2000)

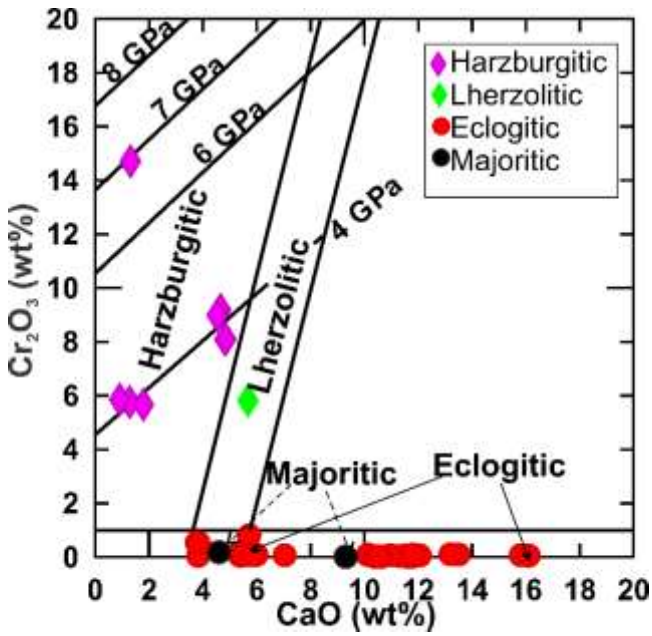

Fig. 2 Cr_2O_3 vs CaO diagram for garnets inclusions in Karowe diamonds. Isobars are from Grütter et al. (2006) and represent minimum pressures (as equilibrium with spinel is not established)

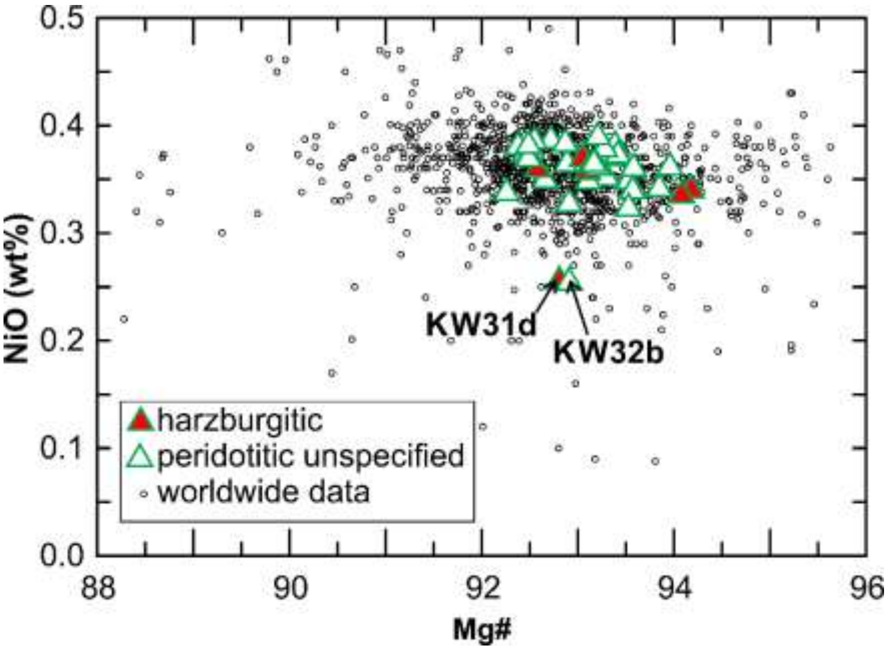

Fig. 3 NiO (wt%) versus molar Mg# (100×Mg/[Mg+Fe]) in olivine inclusions from this study and localities worldwide (n=1,306; Stachel and Harris 2008)

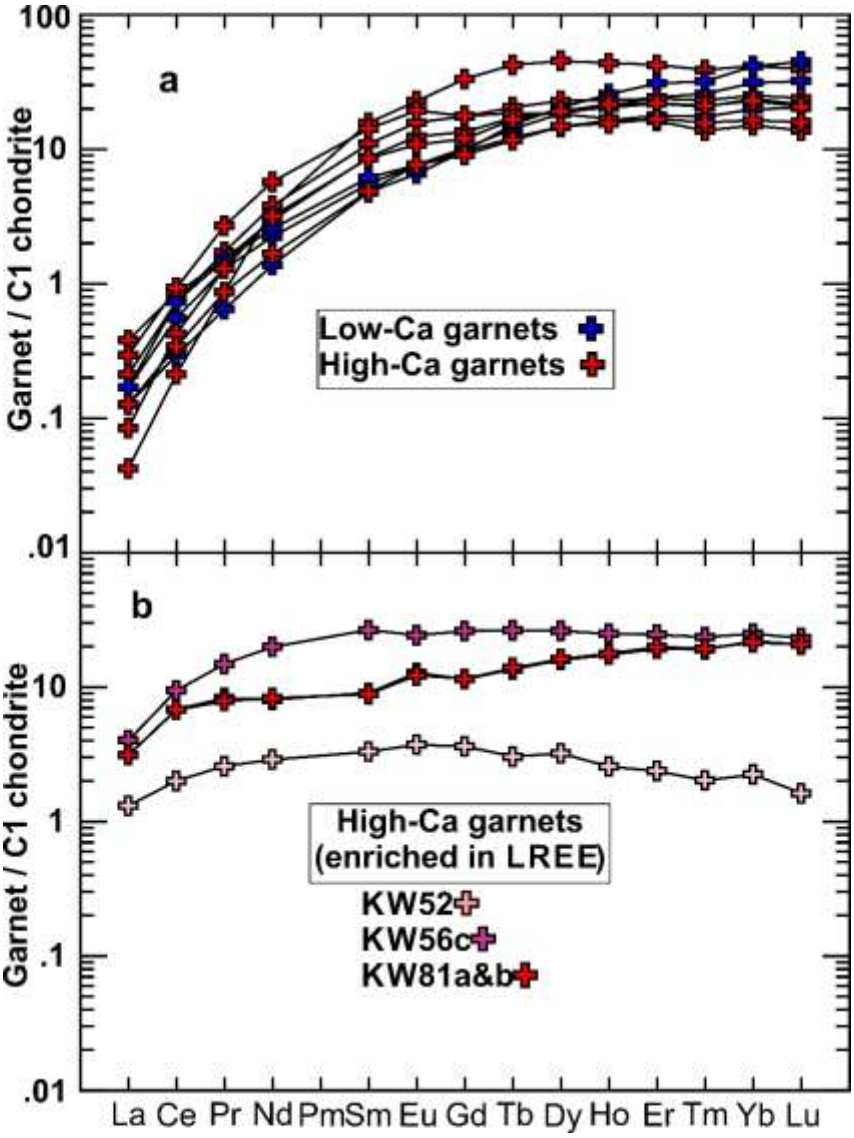

Fig. 4 Chondrite normalized (McDonough and Sun 1995) REE patterns for Karowe eclogitic garnet inclusions. **a**: Low-Ca garnets (n=3) and high-Ca garnets (n=6). **b**: Second group of high-Ca garnets with nearly flat REE patterns

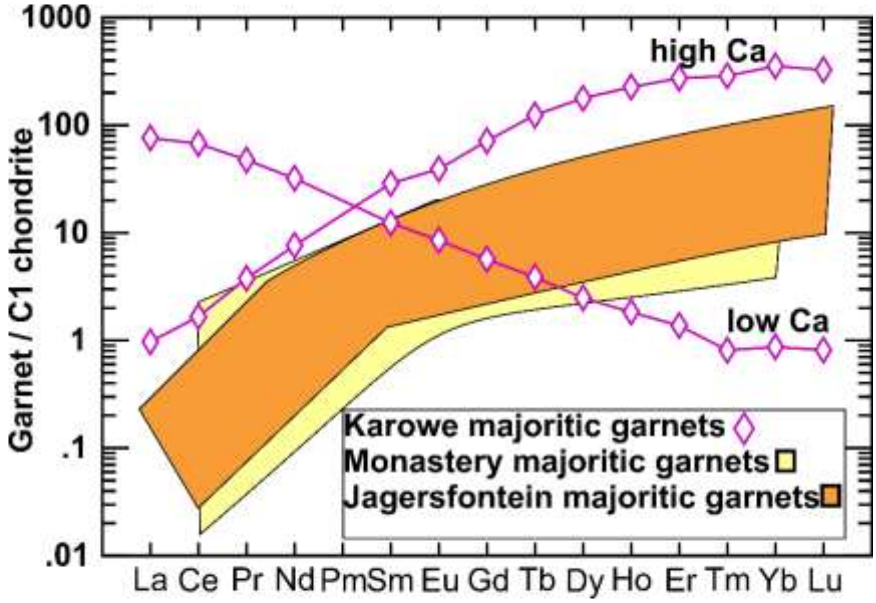

Fig. 5 Chondrite normalized (McDonough and Sun 1995) REE patterns of low- and high-Ca majoritic garnets from Karowe compared to majoritic garnets from Monastery (Moore et al. 1991) and Jagersfontein (Tappert et al. 2005).

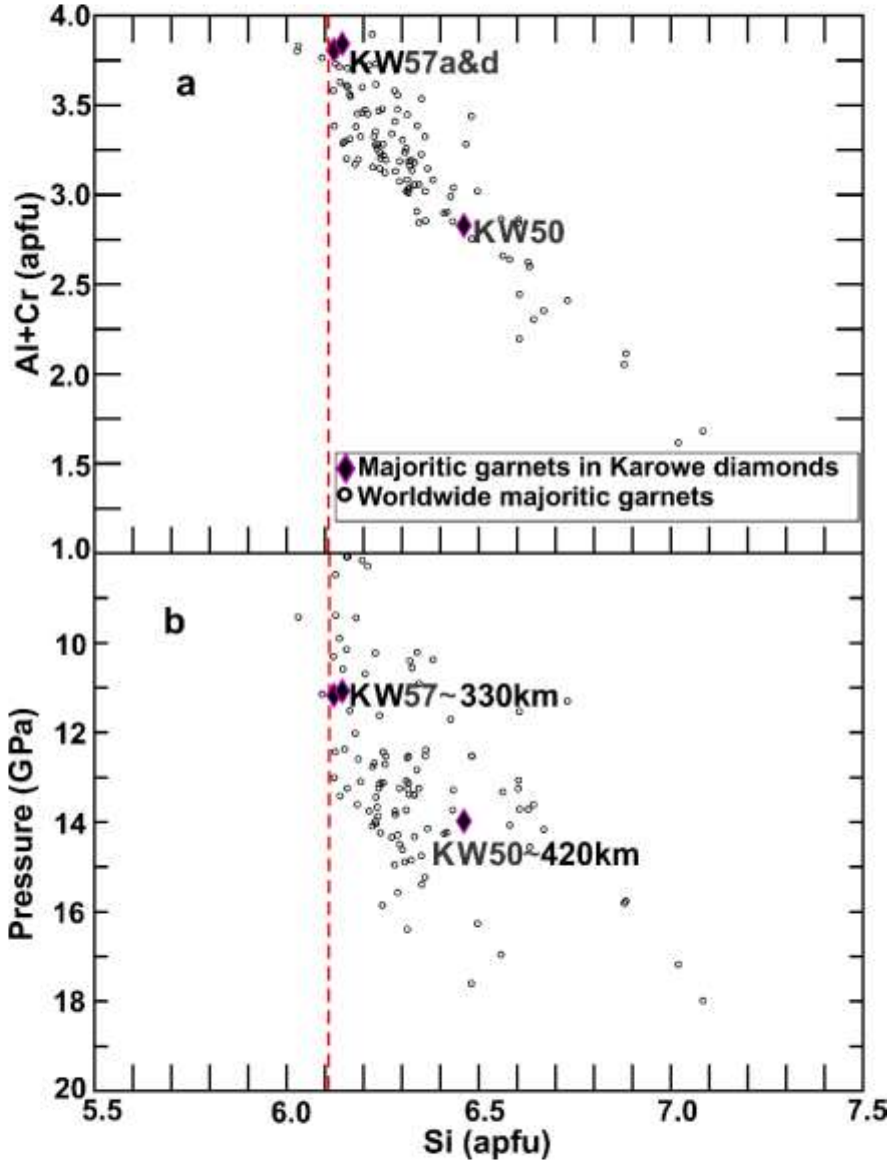

Fig. 6 a: Al+Cr versus Si as atoms per formula unit (apfu, with [O]=24) in majoritic garnets inclusions from Karowe and worldwide sources (n=69; database of Stachel and Harris 2008). Red dashed line indicates threshold value of > 6.12 apfu Si used to define majoritic garnets. **b**: Si apfu plotted against pressure (GPa), calculated using the barometer of Beyer and Frost (2017)